

BACHELOR

Investigating torsion stiffness of protein complexes

Nguyen, T.Y.N.

Award date:
2013

[Link to publication](#)

Disclaimer

This document contains a student thesis (bachelor's or master's), as authored by a student at Eindhoven University of Technology. Student theses are made available in the TU/e repository upon obtaining the required degree. The grade received is not published on the document as presented in the repository. The required complexity or quality of research of student theses may vary by program, and the required minimum study period may vary in duration.

General rights

Copyright and moral rights for the publications made accessible in the public portal are retained by the authors and/or other copyright owners and it is a condition of accessing publications that users recognise and abide by the legal requirements associated with these rights.

- Users may download and print one copy of any publication from the public portal for the purpose of private study or research.
- You may not further distribute the material or use it for any profit-making activity or commercial gain

Take down policy

If you believe that this document breaches copyright please contact us providing details, and we will remove access to the work immediately and investigate your claim.

Investigating torsion stiffness of protein complexes

T.Y.N.Nguyen

MBx 2013-04

Supervisors:

F.A.Gutiérrez-Mejía, M. Sc

Dr. L. J. van IJendoorn

Molecular Biosensors for Medical Diagnostics,
Department of Applied Physics,
Eindhoven University of Technology

Abstract

Specific detection of target biological molecules is an important aspect of biosensors applications. In this study the mechanical properties of a protein complex is investigated with the prospect to gain more knowledge about the aspect of specificity of biosensors. Due to the presence of a small magnetic moment of a superparamagnetic particle, which is bound to a protein complex, mechanical forces can be exerted onto the system. The torsion stiffness of the biological complex can then be investigated.

A rotating magnetic field, which is generated by a quadrupole electromagnet, is used to applied a torque. In order to visualize the rotation motion of the magnetic particle which is bound to a protein complex, fluorescent labels are utilized. Matlab software is used to analyze the rotation motion of the particle.

At first the Troponin – Anti-troponin complex is characterized for posterior use in torsion experiments. The protein troponin is sandwiched between two antibodies specific for two different regions of troponin I. From the dose response curve of the complex, it is observed that there is a high fraction of bound beads at low concentration of the antibodies. It is not clear if these bonds are specific or non-specific. Therefore the Troponin – Anti-troponin complex was not used for the rotation experiments.

In this study the torsion stiffness of the protein G-IgG complex, which is sandwiched between a magnetic particle and a substrate, is investigated. The rotation of the bound magnetic particle is observed to change gradually when the rotating magnetic field strength is increased. The torsion constant of the biological complex is determined by using the rotational Brownian motion analysis. For the measurement with the Brownian motion, an average torsion constant of $(10 \pm 2) \times 10^{-18} \text{ Nm} \cdot \text{rad}^{-1}$ is found. This value is comparable to the value found in literature which is $(6 \pm 2) \times 10^{-18} \text{ Nm} \cdot \text{rad}^{-1}$. This suggests that the rotational Brownian motion analysis can be a valid method for determining the torsion constant of a protein complex. There is another method for determining the torsion constant of the protein complex. This method made use of a rotating magnetic field and by measuring the maximum angle of a bead for a given torque in a rotating magnetic field, torsion constants of the protein G-IgG complex can be determined. For this method the magnetic property of the superparamagnetic bead has to be taken in account.

The protein G-IgG complex is also investigated upon exposure to the surfactant SDS. The torsion constant of the complex decreased when surfactant is added. This indicates that the biological system became less rigid upon exposure to a surfactant.

Table of Contents

1.	Introduction	1
2.	Magnetic properties of superparamagnetic beads	2
2.1	Superparamagnetic beads	2
2.2	Locked magnetic moment	4
2.3	Rotation of a bound bead in a rotating magnetic field.....	5
2.4	Remagnetization of magnetic moment	5
3.	Biological systems	7
3.1	Antibody structure	7
3.2	Protein Troponin – Anti-troponin complex.....	7
3.3	Protein G-IgG complex	9
3.4	Sodium dodecyl sulfate detergent.....	9
4.	Experimental	11
4.1	Bead functionalization	11
4.2	Dose response curve of Tn – anti-Tnl complex.....	11
4.3	Sample preparation of G-IgG complex.....	12
4.4	Magnetic quadrupole.....	13
4.5	Determining the torsion constant of a protein G-IgG complex	14
4.6	Microscope.....	15
4.7	Data analysis	15
5	Results and discussion	17
5.1	Dose response curve of Tn – anti-cTnl.....	17
5.2	Torsion constant of the protein G-IgG complex	18
5.2.1	Determining the torsion constant of the G-IgG complex using rotational Brownian motion analysis	18
5.2.2	Oscillating behavior and effect of magnetic field strength.....	20

5.2.3	The field dependence of the permanent magnetic moment and the angle dependence of the torsion constant.....	23
5.2.4	Influence of surfactant on the torsion constant of the protein G-IgG complex.....	26
6	Conclusions and outlook.....	29
7	References	30
8	Appendix	31

1. Introduction

A biosensor is a device that measures the concentration of biological molecules in fluid. The principle of a biosensor is based on detection of biomarkers e.g. protein. Research in biosensors field has grown rapidly since its beginning about 20 years ago. Biosensors promise to become an essential tool for early detection and prevention of diseases and prescription of valid treatments. The development of biosensors requires an accurate and specific detection of low concentration of biomarkers in a small amount of time. Besides there is also a need for a so-called point-of-care approach. This means that tests with biosensors need to be performed close to the patient to reduce time and travel costs.

Since recent years there is a new development in the biosensor research that focuses on application of magnetic particles, in particular superparamagnetic particles, for detection of biomarkers. The magnetic particles are composed of a polystyrene matrix with ferrimagnetic grains. In the absence of a magnetic field, there is no net magnetization of the superparamagnetic bead. But when an external magnetic field is applied, the superparamagnetic particle will have a net magnetization. This will be discussed in chapter 2.

The magnetic properties of these particles allow researchers to investigate mechanical properties of biological systems. The superparamagnetic particles are able to capture target molecules when they are functionalized with biological complementary molecules. The nature of the molecular complexes used in this research will be described in chapter 3. By applying a magnetic field, the beads will act as mechanical transducers so that mechanical forces can be applied on the biological system. In this research the superparamagnetic particles (also called beads) are used to investigate the twisting of protein complexes. By coating the beads with proteins, they can be used to capture target molecules so that these molecules are sandwiched between the bead and a surface as illustrated in

Figure 1. 1. The technical aspects of the technique will be addressed in chapter 4.

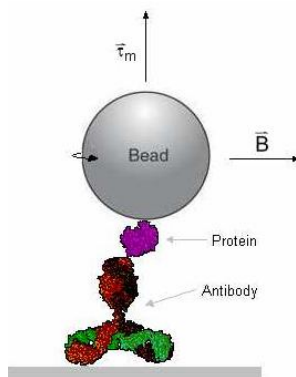


Figure 1. 1: Schematic representation of the biological system studied in this research. The protein is sandwiched between the superparamagnetic bead and a surface coated with antibody.

The characteristics of the biological system such as the torsion stiffness can be studied by investigating the angular displacement of the magnetic bead. Besides measurements with an external magnetic field, the rotational Brownian motion analysis is also used for characterizing the torsion constant of the biological system in absences of magnetic fields. Examples of measurements of the torsion constant of protein complexes are shown in chapter 5. Finally, the conclusions and outlook of this work will be given in chapter 6.

2. Magnetic properties of superparamagnetic beads

Dynal beads carboxyl M-270 (Invitrogen) particles are used in this research to generate a magnetic torque on protein complexes. When a rotating magnetic field is applied, due to their magnetic properties, magnetic forces can be exerted on them. In this chapter these properties will be discussed.

2.1 Superparamagnetic beads

The M-270 particles used here consist of 6-12 nm magnetic nanoparticles in a polystyrene matrix. These magnetic nanoparticles, or grains, are made of magnetite (Fe_3O_4) which is a ferrimagnetic material. The magnetic grains inside the bead have an uniaxial anisotropy and are in single domain state which means that each grain has a uniform magnetization orientation and a single magnetic moment.

The bead with the polystyrene matrix and grains are schematically illustrated in Figure 2. 1.

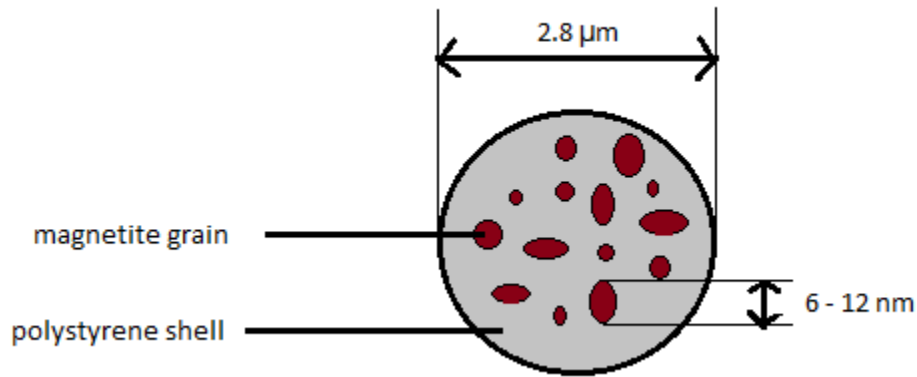


Figure 2. 1: Schematic representation of the superparamagnetic bead. Magnetite grains with diameter of 6 – 12 nm are embedded within a polystyrene matrix.

The magnetization of each grain in the bead has a preferential direction. This phenomenon is called magnetic anisotropy. In the crystal structure of magnetite, the preferential direction is in the $\langle 111 \rangle$ direction and is also called the easy axis. There is a hard axis in the $\langle 100 \rangle$ direction and also an intermediate axis in the $\langle 110 \rangle$ direction. In order for the magnetization to rotate from the easy axis to the hard axis energy is required. This energy is called magnetocrystalline or anisotropy energy. Thermal fluctuations can cause the magnetization to change direction. The required energy for flipping is KV , where K is the anisotropic constant and V is the volume of the particle. For paramagnetic materials the direction of magnetization of a single grain can change direction thermally. A typical flipping time for the magnetization direction flip and reverses its direction is:

$$\tau = \tau_0 \exp\left(\frac{KV}{k_B T}\right). \quad (2.1)$$

Here τ_0 is the attempt time and its reciprocal is the attempt frequency. τ_0 is typically 10^{-9} - 10^{-10} s [1]. k_B is the Boltzmann constant and T is the temperature. The anisotropy constant K is in the order of $1 * 10^4$ J/m³ to $5 * 10^4$ J/m³ [2].

When the flipping time is longer than the timescale of the experiment, the magnetization of a grain is considered to be fixed. Assuming that the temperature and the anisotropy are constant, a bead will

show paramagnetic behavior for magnetic grains with a diameter below a certain critical size limit. This limit corresponds to the smallest grain size for which the magnetization of the grain is still fixed on the timescale of the experiment. The experiments described in this report are performed with a rotating magnetic field with frequency in the order of 1 Hz corresponding to a characteristic timescale of 1 second.

In Figure 2. 2 the flipping time of the magnetic moment in the grain is plotted as a function of the diameter of the particle.

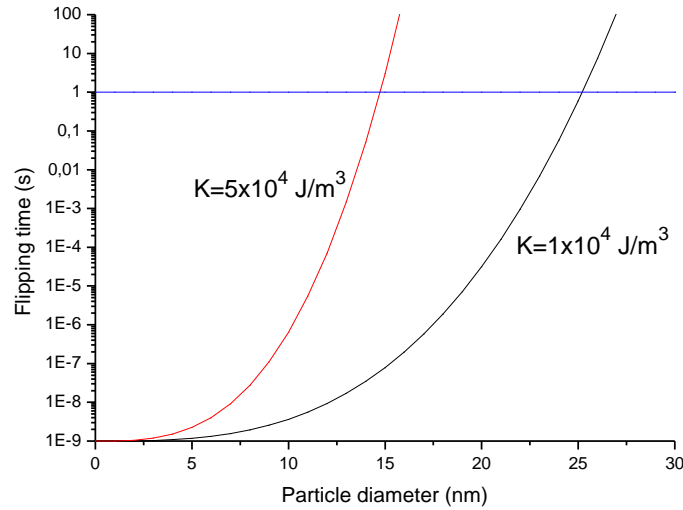


Figure 2. 2: The flipping time of a magnetite grain as a function of the particle diameter. The horizontal blue line represents a flipping time of 1 second.

The flipping time of one second is found for grains with radius between approximately 14 and 25 nm. This range is considered as the critical size limit of the magnetic grains. Since the typical diameter of the grains in the beads are only 6 to 12 nm, the beads treated here show a paramagnetic behavior. In paramagnetic material the individual magnetic moment is created by a single atom while in the magnetic bead the magnetic moment is a combination of all aligned spins within a single domain. As a consequence the magnetization of the magnetic bead used for this study is much larger than the magnetization of paramagnetic material. The magnetic beads can thus be considered superparamagnetic.

The direction of the easy axis of a grain is random so that the net magnetization of a ensemble of the grains (the bead) is zero. When averaging over time, the magnetization of the superparamagnetic bead is also zero since the flipping time of the grains is equal for both directions of the easy axis.

When an external magnetic field B is applied, the interaction between the magnetic moment of the magnetite grains and the magnetic field has to be taken in account. The flipping time for both directions of the easy axis is no longer equal. Assuming that the easy axis of the grain is directed parallel to the magnetic field, two different flipping times are exhibited:

$$\tau = \tau_0 \exp\left(\frac{KV \pm mB}{k_B T}\right) \quad (2. 2)$$

where m is the magnetic moment of the magnetite grain.

In the case that the magnetization is aligned with the magnetic field, it takes the magnetization more time to flip than in the case of an opposite alignment. As a result, there is a nonzero net magnetization

in the direction of the external magnetic field. In our case an ensemble of ferrimagnetic grains (the bead) is able to exhibit superparamagnetism. The magnetic response of a superparamagnetic bead as a function of the magnetic field can be described by the Langevin-function L:

$$M = nmL\left(\frac{mB}{k_B T}\right) = nm\left(\coth\frac{mB}{k_B T} - \frac{k_B T}{mB}\right). \quad (2.3)$$

Here m is the magnetic moment of the individual grains and n is the total number of magnetic grains in the ensemble. Note that in this model all grains are assumed to be identical when a M-270 bead contains of a distribution of different grain sizes. Some of the larger grains will have a diameter larger than superparamagnetic diameter. Therefore the flipping time of the magnetization could be longer than the characteristic time scale of the measurement. This means that an ensemble of these grains behave ferromagnetically and show a spontaneous magnetization.

2.2 Locked magnetic moment

As discussed above, the direction of the magnetization of a superparamagnetic bead aligns with the applied magnetic field. Therefore, no torque is expected to work on the bead. However, several studies [2], [3] and [4] showed that a torque can be applied to the bead. This implies that the bead has a small locked magnetic moment μ_{locked} . Experimentally, the locked magnetic moment can be determined by two methods.

The first method is based on finding the balance between the viscous torque of the bead in fluid, which increases with the angular bead velocity, and the maximum magnetic torque applied by a rotating magnetic field. The permanent magnetic moment will enable the bead to follow the rotating field while the viscous torque will oppose the bead to follow the field. The magnetic torque is given by:

$$\vec{\tau}_m = \vec{\mu}_{locked} \times \vec{B} = \mu_{locked} B \sin\varphi \quad (2.4)$$

with φ is the phase lag between the magnetic moment and the magnetic field.

The viscous torque is given by:

$$\tau_{visc} = -8\pi\eta R^3 \frac{d\theta}{dt}. \quad (2.5)$$

Here η is the dynamic viscosity of water, R is the radius of the bead and θ is defined as in Figure 2. 3.

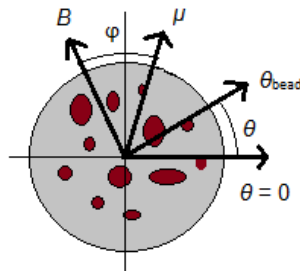


Figure 2. 3: A schematic draft of a magnetic particle. The angle of the bead and the phase lag between the magnetic moment and the magnetic field are shown as well as the direction of μ and B .

The torque balance for a particle is given by:

$$\mu_{\text{locked}} B \sin \varphi = 8\pi\eta R^3 \frac{d\theta}{dt}. \quad (2.6)$$

At low frequencies, the locked magnetic moment of the bead is able to follow the field. But as the frequency increases, the viscous torque increases as well. At a certain frequency the viscous torque is larger than the magnetic torque at its maximum. Consequently the bead cannot follow the field any longer leading to a decrease in rotation frequency. This certain frequency is called the breakdown frequency ω_{bd} . By measuring the breakdown frequency the maximum magnetic torque can be determined. As this torque depends on the locked magnetic moment of the bead, the locked magnetic moment can be determined as well.

The second method is based on the rotational Brownian motion of a superparamagnetic bead in a static magnetic field. The rotational motion of the bead is restricted in the direction of the static magnetic field. This is due to the tendency of the system to minimize its potential energy. The restricted rotational motion depends on the magnitude of its magnetic moment. As a consequence, a Brownian motion analysis can be used to determine the locked magnetic moment of the bead.

Verhees [3] has determined the value of the locked magnetic moment using both methods. The values found from both methods are in agreement. The locked magnetic moment of the M-270 Dynabead is in the order of 10^{-16} Am^2 .

2.3 Rotation of a bound bead in a rotating magnetic field

In this paragraph the magnetic rotation of a bead that is bound to a surface via a biological complex is described. Besides the viscous and magnetic torque described above, the bead also experiences a resistant force due to the stiffness of the biological system which consists of a protein ligand-receptor pair. This system can be seen as a rotational spring and the torsional stiffness can be considered as a torsional spring k . As the viscous torque, the torque due to the biological system also tries to restrict the bead to move along with the rotating field. The torque balance of equation (2.6) becomes:

$$\mu_{\text{locked}} B \sin \varphi = 8\pi\eta R^3 \frac{d\theta}{dt} + k\theta. \quad (2.7)$$

In the absence of the rotating magnetic field, the system will stay at a fixed angular position. This angle is set as the equilibrium position $\theta = 0$. When a rotating magnetic field is applied the bead will rotate from its equilibrium angle and initially follow the field. When $\varphi = 90^\circ$ the magnetic torque reaches its maximum and starts to decrease. The bead rotates then backward due to the torsional spring of the system. An accelerated backward rotation also appears when the phase lag passes 180 degrees. The magnetic torque is now in the same direction as the torque induced by the biological system.

2.4 Remagnetization of magnetic moment

The grains in a superparamagnetic bead have a distribution in magnetic moment orientation and also a distribution in grain size. The orientation distribution is not random since the bead has a net magnetization. The effective magnetic moment is described by the distribution of the magnetic moments of the grains inside the bead. Depending on the phase difference between individual magnetic moment and the coercive field of individual grain, the magnetic moment of the grain can remagnetize. For individual grain, remagnetization occurs when the applied magnetic field exceeds the coercive field of the grain. This means that the magnetic moment of the grain will flip. Note that the coercive field of a grain can be different from the average coercive field of all grains. When a rotating magnetic field is applied, three scenarios of describing the magnetic moment of the bead are possible. Scenario 1: the

coercive fields of the grains are not exceeded so that no remagnetization will happen. The bead will follow the rotating magnetic field with a constant phase lag. Scenario 2: when the field is applied, the coercive field of one of the grains is exceeded resulting in remagnetization of that grain. The grain flips 180° and its magnetic moment opposes the effective magnetic moment. The effective magnetic moment is then reduced, which is illustrated in Figure 2. 4b

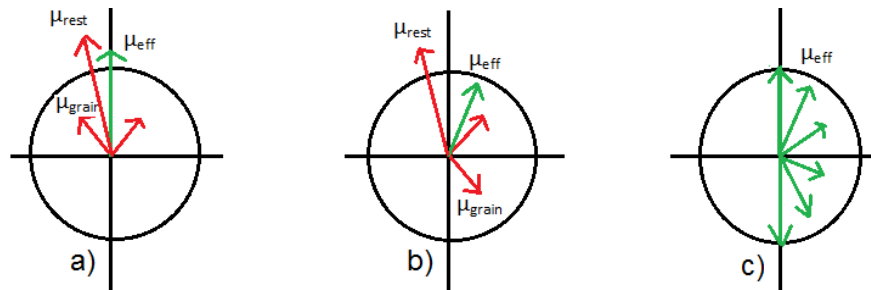


Figure 2. 4: The effective magnetic moment μ_{eff} of the bead and the remagnetization of individual grains. a) the effective magnetic moment is composed of a distribution of individual magnetic moments of the grains. Note that only the moment that remagnetizes first is considered in the description and the remaining magnetic moments are denoted with μ_{rest} . b) situation after the first moment has remagnetized. The magnetic moment now opposes the effective magnetic moment which is changed in direction and reduced in magnitude. c) due to the cascade effect the effective magnetic moment changes magnitude and direction.

The reduced effective magnetic moment leads to a reduced effective magnetic torque of the bead, resulting in a new equilibrium between the magnetic torque and the viscous torque. Corresponding to the new equilibrium, a larger phase difference between the effective magnetic moment of the bead and the field appears. The bead continues to rotate further and when the new phase difference is large enough such that the coercive field of another grain is exceeded, its magnetic moment will remagnetize. In addition, a new equilibrium between the magnetic torque and the viscous torque is induced, corresponding to again a larger phase difference between the effective magnetic moment and the field. When this new phase difference is not large enough such that the magnetic field does not exceed the coercive field of the next grain, this grain's moment will not flip and the bead will continue to follow the rotating field. Scenario 3: when applying the magnetic field, the moments of the two first grains flip as described in scenario 2. But in this case the phase difference after the second grain flipped is large enough such that the moment of the next grain flips. This may induce flipping of more grains which can lead to a cascade effect where all the grains will ultimately remagnetize. Consequently the effective magnetic moment changes direction and when the cascade effect has finished, the effective magnetic moment has flipped 180° compared to its initial position, see Figure 2. 4c. An important implication of the cascade effect is that the maximum magnetic torque can be reached for a phase difference φ smaller than 90° . This means that for a bead bound to the protein G-IgG complex, the bead can rotate backward before a phase lag of 90° is reached.

3. Biological systems

In this chapter, two biological systems that are used in our experiments will be described. The first complex is the Troponin – Anti-troponin complex. The initial aim is to characterize it in particle-based immunoassay for posterior use in torsion experiments. The second complex is the protein G-IgG complex. This biological system will be used to investigate conformational changes of the complex upon surfactants exposure.

3.1 Antibody structure

Immunoglobulin (Ig) or antibodies are proteins produced in blood and are used by the immune system to identify and defend the organism against invasion of bacteria, viruses or foreign agents. An antibody recognizes and specifically binds to a particular substance known as antigen. Subsequently, the immune system is triggered and a number of processes within the immune system will arise to destroy the antigen. A common structure of an antibody is illustrated in Figure 3. 1.

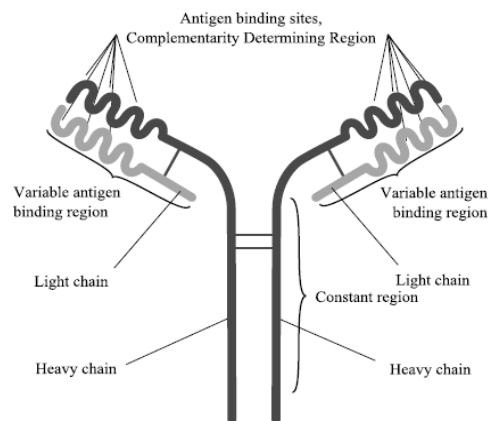


Figure 3. 1: Schematic representation of an antibody. The protein consists of four polypeptide chains; two identical heavy chains and two identical light chains.

The Y-shape of an antibody can be divided in two regions, namely the fragment crystallizable (Fc) region and the fragment antigen-binding (Fab) region which forms the top arms. The Fab fragment can bind specifically to one particular epitope of a particular antigen. The part of an antibody that can recognize the epitope is called paratope. Due to their specific antigen-binding property, the Fab fragment generally differs among different antigens. The Fc region plays a role in modulating cell activity. By binding to specific proteins the Fc region ensures that each antibody generates an appropriate immune response for a given antigen.

3.2 Protein Troponin – Anti-troponin complex

Troponin (Tn) is a protein found in striated (skeletal and cardiac) muscles. It is a sarcomeric Ca^{2+} regulator for muscle contraction and is consisted of three subunit: troponin I, T and C (TnI, TnT and TnC). The crystal structure of troponin is illustrated in Figure 3. 2.

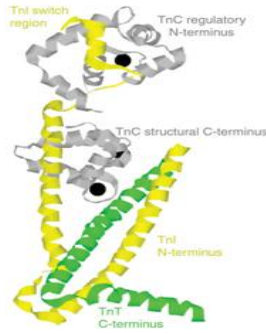


Figure 3. 2: Crystal structure of the troponin core domain. The subunits are also indicated. TnC, TnI and TnT are colored in grey, yellow and green, respectively, with Ca^{2+} colored in black.

The subunit TnC is responsible for conformational rearrangement of the protein troponin under influence of calcium. TnC is a member of the EF-hand family of Ca^{2+} -binding proteins. The protein is consisted of N- and C-terminal globular domains connected by a α -helix, Figure 3. 3.



Figure 3. 3: Structure of a Ca^{2+} -saturated TnC found via x-ray crystal analysis. The two globular regions are connected by a rigid α -helix.

Each domain contains of a pair of helix-loop-helix motifs (EF-hands). A helix-loop-helix motif is characterized by two α -helices connected by a loop. Although all four EF-hands of TnC are meant to bind Ca^{2+} ions, the first one of the cardiac TnC is unable to bind Ca^{2+} . Consequently only the second EF-hand of the N-terminal domain is able to bind Ca^{2+} ions. It is generally accepted that the third and fourth EF-hands of the C-terminal domain play a structural role by anchoring TnC into the troponin complex [5] After binding with calcium TnC undergoes a structural change, Figure 3. 4, so that the protein troponin also experiences conformational rearrangement.

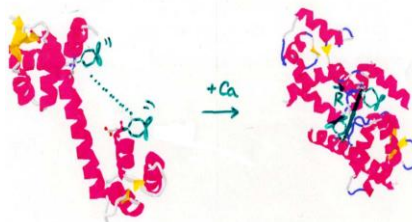


Figure 3. 4: Schematically drawing of TnC after adding calcium. The protein undergoes conformational change.

The information on the conformational changes of TnC under influence of Ca^{2+} has been accomplished by several spectroscopic studies such as X-ray crystallography and NMR [5]. In this work we will form an immunoassay with antibodies specific for two different regions of troponin I, namely anti-troponin I1 and anti-troponin I2.

3.3 Protein G-IgG complex

Immunoglobulin G (IgG) is one of the most important proteins in the biological sciences. It represents 75% of serum immunoglobulin in humans. Measurements of immunoglobulin G can be used for diagnosis of certain conditions.

Group C and G Streptococci are bacteria which produce a range of toxins and surface proteins that combat the human immune system and also cause diseases. Protein G from group C and G Streptococcal species is a cell-surface protein that bind selectively to the Fc fragment of IgG [6] A. E. Sauer-Eriksson, G. J. Kleytwegt, M. Uhlén, T. A. Jones. Crystal structure of the C2 fragment of streptococcal protein G in complex with the Fc domain of human IgG. Structure 3: 265-278, 1995.. The domain which is responsible for binding to IgG is consisted of one α -helix that is linked with a four-stranded β -sheet. The IgG binding region of protein G is located at the C-terminal end of the molecule. Figure 3. 5 shows the domain B1 of protein G which binds to IgG.

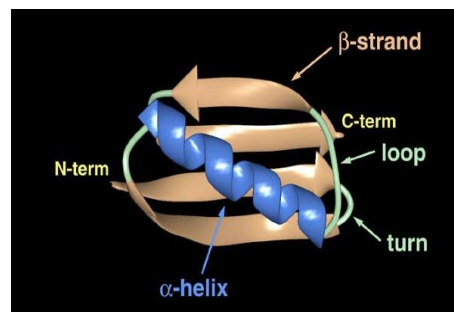


Figure 3. 5: Immunoglobulin binding domain of protein G.

It has been reported that the interaction between protein G and the Fc fragment of IgG is related to charged and polar contacts [6]. Protein G also has a weak interaction with the Fab region of IgG. However, the affinity of protein G for binding with Fab region is just 10% of its affinity for binding to Fc region.

3.4 Sodium dodecyl sulfate detergent

An anionic surfactant is an amphiphilic molecule consisting of a hydrophobic tail and a negatively charged hydrophilic head. For the experiments described in this report, Sodium dodecyl sulfate (SDS) anionic surfactant is used. The structure of SDS is shown in Figure 3. 6.

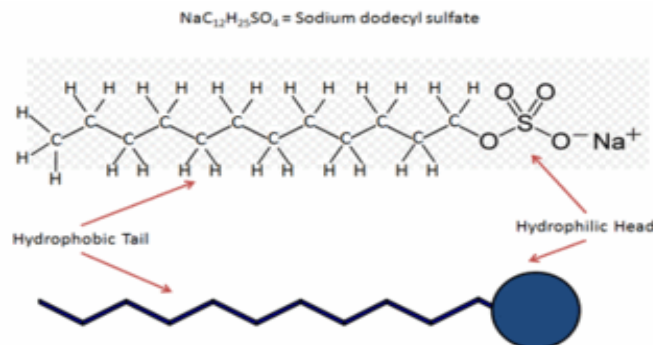


Figure 3. 6: Schematic representation of SDS surfactant. The hydrophilic head and the hydrophobic tail are also indicated.

At high concentrations detergent monomers aggregate into structures called micelles. A micelle is a thermodynamically stable aggregate of detergent monomers. In a micelle the hydrophobic tails are sequestered inward avoiding exposure to water while the hydrophilic heads are oriented outward in contact with water. The range of detergent concentration above which micelle form is called the critical micelles concentration (CMC). Additional surfactants added to the system will go to micelles.

In biochemistry SDS is widely used as denaturant e.g. for SDS Polyacrylamide gel electrophoresis (PAGE). SDS denatures proteins by binding to the protein chain with its hydrocarbon tail and coating the chain with surfactant molecules. It is also know that SDS can cause structural changes in proteins. Therefore in this research SDS is added to protein complexes to detect systematic changes in their the torsion constant.

4. Experimental

The immunoassay of the troponin system is investigated by means of a dose-response curve. The assay will be explained in section 4.2. The twisting of the protein G-IgG complex is investigated by using the M-270 particles. The materials and methods that are used for the experiments will be discussed in this chapter.

4.1 Bead functionalization

Both the protein complexes that are used for the experiments are sandwiched between a superparamagnetic bead and a surface coated with antibodies. The surface of the M-270 beads contains carboxylic end-groups. Protein molecules bind covalently to the carboxylic end-groups of the bead, forming peptide bonds. Via a so-called EDC-NHS reaction these end-groups can be exploited to bind to any protein directly. Coating the M-270 beads with proteins and streptavidin is accomplished following the EDC-NHS reaction scheme. First, 1-Ethyl-3-(3-dimethylaminopropyl)carbodiimide (EDC) interacts with the carboxylic end-groups forming highly active but unstable EDC groups. To stabilize N-Hydroxysuccinimide (NHS) is added and substituting EDC. NHS esters are then formed. Before adding the protein solution, a washing step is required to remove the free EDC in the solution. This is to prevent reactions of free EDC in the solution and the carboxylic end-groups of the proteins. After the washing step the proteins are added en due to the amine end-groups of the proteins, the NHS is replaced by the proteins. At last ethanolamine is added to quench the free carboxylic end-groups so that non-specific bonds of the functionalized beads can be minimized. The EDC-NHS reaction scheme is shown in Figure 4. 1.

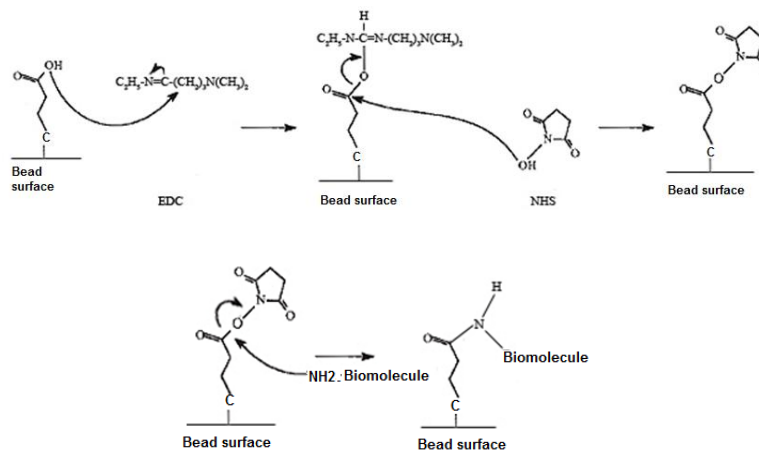


Figure 4. 1: The EDC-NHS reaction scheme. This reaction is used for binding of protein and streptavidin to the magnetic beads. First the EDC molecule replaces the hydrogen atom of the carboxyl end-group. After that a NHS molecule substitutes the unstable EDC group. In turn the NHS molecule is then substituted by the amine end-group of a protein.

4.2 Dose response curve of Tn – anti-TnI complex

To evaluate the sandwich assay of the protein complex we choose the following configuration: anti-troponin I (anti-TnI1) (HyTest 560) – cardiac troponin complex ICT (Hytest 8IC63) and anti-troponin I (anti-TnI2) (Hytest 19C7) as can be seen in Figure 4. 2.

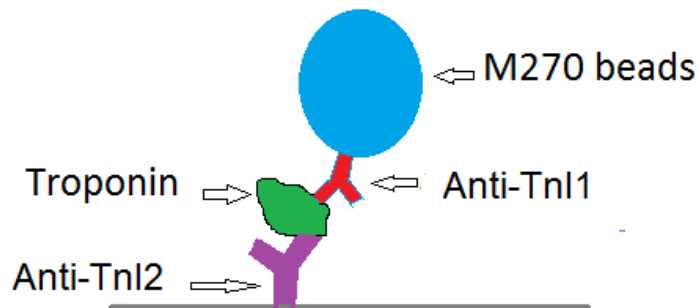


Figure 4. 2: Sandwich bead assay for the protein troponin complex. The protein troponin is sandwiched between two anti-TnI with specificity for two different sites of TnI.

The superparamagnetic particles are coated with a biological complex of anti-troponin I (anti-TnI1) and troponin. The anti-TnI1 binds covalently to the beads using the EDC-NHS reaction as described in the previous section. The paratope of the anti-TnI1 recognizes the epitope on the surface of troponin.

In order to make a sandwich immunoassay, substrates coated with anti-troponin I2 (anti-TnI2) molecules are prepared. Anti-TnI2 can bind to the substrate through physisorption which is caused by the Van der Waals forces. 18x18 mm² polystyrene and glass coverslips (VWRinternational, Radnor, PA) are used. The substrates are thoroughly washed by sonication steps of 5 minutes with acetone followed by isopropanol. After that the cover slips are dried for another 5 minutes in a vacuum desiccator. To create a fluid cell for the measurements a Secure-Seal™ imaging spacer has been attached to each cover slip. After washing the substrates, incubation of antibodies can be performed. In order to obtain the dose response curve, different dilution series of anti-TnI2 are prepared and incubated onto the substrates. Incubation happens by physisorption at room temperature for 45 minutes. Protein troponin can also bind directly to the substrates. To prevent bonds of troponin to the glass substrates, Bovine serum albumin (BSA) is used as blocking agent to diminish non-specific absorption of troponin. BSA is diluted in 100 nM Phosphate buffered saline (PBS) blocking buffer. Before the protein solution is added, 100 µl of blocking buffer is incubated onto the substrate at room temperature for one hour. After that the substrates are ready for the experiments. Before the measurement 8.5 µl of solution consists of beads coated with anti-TnI1 and troponin is pipetted onto another glass substrate. The cover slip is then turn upside down and placed onto the glass substrate coated with antibody. Incubation of the coated bead on the antibody coated substrate takes 5 minutes. The sample is then turn upside down so that the unbound beads will be separated from the bound beads. By focusing the microscope at the bottom of the fluid cell and on the functionalized substrates, the fraction of beads that are bound via the Tn – anti-TnI can be computed. To obtain the dose response curve, the number of bound beads on the top substrate and the number of free beads on the bottom are counted by using Matlab algorithms.

4.3 Sample preparation of G-IgG complex

Apart from the Tn – anti-TnI complex, the biological protein G-IgG complex is also investigated. The torsion constant of this system in 100 nM PBS solution is measured with different magnetic field strengths with the method described in the next section. To investigate the influence of detergent on the torsional properties of the system, solutions with different concentrations of surfactant is used for the measurements. The torsion constant from these measurements are determined as well. The rotational Brownian motion analysis is also used for determining the torsion constant.

The beads are coated with protein G and streptavidin and to visualize angular rotation of the bead, biotin-labeled fluorescent particles (Fluo-Spheres, biotinylated, yellow/green, 0.2 µm diameter) purchased from Invitrogen Carlsbad, CA are used. These particles have an emission peak respectively

around 505 and 515 nm. When excited, these particles will give a green-yellow color [2]. Protein G-IgG complex is sandwiched between the superparamagnetic bead and glass coverslip. Glass substrates are used for the experiments with G-IgG complex instead of polystyrene. Van Reenen [2] showed that the polystyrene substrate has autofluorescence due to emission bands in the 330-520 nm wavelength region. The overlapping in emission region of the fluorescent particles and polystyrene substrates leads to a blurred image of the bead when view under a microscope.

The washing steps described from the previous section are also applied for the glass substrates (22x22 mm²) of the experiments described in this section. The glass substrates are coated with antibody IgG via physisorption. In this study an IgG concentration of 1 nM is used to decrease the probability of multiple bonds. A 100 μ l droplet of IgG antibodies are incubated at room temperature for 45 minutes. Similar to the preparation of the troponin complex, before adding the protein solution 100 μ l of blocking buffer is used. The orientation of the bonds of IgG molecules on glass is random. This means that some IgG molecules will be lying on their side, some will bind to glass via their paratope regions and some will bind via their Fc fragment. Protein G is known to bind specifically to the crystallizable part (Fc) of the antibody. Consequently the fraction of IgG that is able to bind protein G will be low. Additionally due to the randomness of bound IgG molecules, protein G can bind to the Fc fragment of a standing IgG molecule or to the Fc part of a IgG molecule that is lying on the side. This leads to different orientation and bond types of the biological system. Because of the difference in binding structure of the protein G-IgG complex, a variation in the torsion constant of the complex can occurred. The blocking buffer is incubated for one hour and then 45 μ l of the beads coated with protein G solution is incubated onto the glass substrate coated with IgG. To align the locked magnetic moment of the beads, the incubation step of the protein solution is performed in the presence of a 2mT static magnetic field. Before the incubation a demagnetization step is required to remove any remnant field in the magnetic quadrupole setup, which is described later on in this report. The incubation takes 10 minutes. For this experiments a closed fluid cell (Fluid cell R-20 fluidic chamber, 358 μ l volume, Warner Instruments, Hamden, CT) is used, Figure 4. 3.



Figure 4. 3: Closed fluid cell used for the experiments.

A clean glass substrate is glued to the back of the fluid cell using a synthetic grease. The fluid cell is then mounted on the magnetic quadrupole. The glass substrate on which the mixture of beads solution locates is turned upside down and placed onto the top of the fluid cell. The unbound beads will sediment to the bottom due to gravity and the bound beads will stay at the top. With the fluid cell of Figure 4. 3 the solution in the fluid cell can be exchanged. On the sides of the cell, there two small holes. A small hose connected with the desired solution can be stuck into one of the holes. The solution can now be pumped into the fluid cell via the hose. This way, detergent can be added to the fluid cell.

4.4 Magnetic quadrupole

As the superparamagnetic beads have a locked magnetic moment, a magnetic torque can be applied on them. The magnetic torque is caused by a rotating magnetic field generated by a magnetic quadrupole which is developed by Janssen *et al.* [4]. With this device a uniformly rotating magnetic field, that

actuates the beads in a horizontal plane, is generated. The quadrupole is consisted of four coils placed in the corners of a square located on a polystyrene frame, see Figure 4. 4

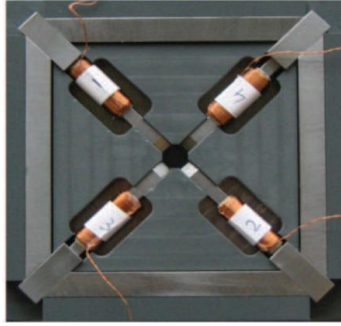


Figure 4. 4: Top view of the magnetic quadrupole with four electromagnets.

Inside the coils soft iron cores are placed to increase the magnitude of the rotating magnetic field. To generate a rotating and horizontal magnetic field at the center, the applied sinusoidal currents through the neighboring coils has a phase difference of 90 degrees, while for the opposite coils the phase difference is 180 degrees. Both the alternating currents are connected with two identical function generators (Agilent 33250A). A controller between the coils and the function generators converts the synchronized output voltage into a current which passes through the coils. The controller is powered by an Agilent 6622A power supply. The function generators and the power supply are controlled via a computer.

In order to obtain a rotating magnetic field, gradients in the center of the quadrupole has to be minimized in both horizontal and vertical direction. It has been reported that by slanting the tips of the cores under 45 degrees the smallest gradient is obtained [2]. This constant horizontal gradient near the center is measured to be smaller than 0.25mT/mm up to a distance of 5 mm from the center of the quadrupole. There is also a vertical gradient since the heights of the samples and the electromagnets are not equal. The vertical gradient is measured to be 1.5 mT at its maximum and pointed downward. The magnitude of the force which is exerted onto the magnetic beads due to the vertical gradient is comparable to the gravitational force.

The field strength and rotation frequency are controlled by a LabView software that is written [7]. Demagnetization and incubation are performed using this software. Demagnetization is carried out by a sinc-shaped current that passes through four coils with a magnetic field strength of 20mT at a user-defined frequency. Incubation is performed with a 2 mT static magnetic field for 10 minutes. Rotating magnetic field with different field strengths and frequencies are generated and controlled by this software.

4.5 Determining the torsion constant of a protein G-IgG complex

The torsion constant of the biological system can be determined by two different methods as previously mentioned. The first method is to determine the maximum angle of the bead. The maximum angle θ_{\max} is defined as the angle from the equilibrium at which the bead reverses its rotation from forward to backward. The bead velocity at θ_{\max} is zero. By determine θ_{\max} the torsion constant k can be calculated with equation (4.1)

$$k = \frac{\mu_{\text{locked}} B \sin \varphi}{\theta_{\max}}. \quad (4. 1)$$

The second method is based on the rotational Brownian motion analysis. In a fluid the particle will show fluctuations in angle position due to thermal collisions. This is called the rotational Brownian motion. A molecular torque will try to bring the particle back to its equilibrium position by applying a restoring force. When the torsional spring is approximated by a harmonic oscillator, the potential energy of the biological complex is:

$$U = \frac{1}{2}k\theta^2. \quad (4.2)$$

Here θ is the angular deviation from the equilibrium.

The probability to find the particle at a certain angle depends on the ratio between potential energy of the system and the thermal energy. The distribution function which gives the number of beads at a certain angle is given by equation (4.3):

$$P(\theta) = \exp\left(-\frac{k\theta^2}{2k_B T}\right). \quad (4.3)$$

Here k_B is the Boltzmann constant and T is the temperature.

The torsion constant can be determined by recording the rotational motion of the biological system in the absence of the external magnetic field. Histograms can be made from the time traces obtained from the measurements. By using equation (4.3) to fit the histogram results of the measurements, k can be determined.

4.6 Microscope

The microscope that is used for the experiments is a Leica DM6000M. It has a 63x immersion objective and in combination of a 10x (and a possible 2x) magnifying lens, the microscope achieved a magnification of 1260x. The bead motion is recorded with a 528 x 512 pixels Andor Neo sCMOS camera. A frame rate of 33 frames per second and an exposure time of 0.33 second are used for the measurements. A typical measurement consists of 2000 frames. A mercury lamp is used to visualize the beads and a filter cube in reflective mode is used to illuminate small fluorescent particles.

4.7 Data analysis

The number of bound beads is counted by using Matlab algorithms. In the beads counting algorithms, the size of a selected bead is determined. The algorithms then search for beads with the same size and give a total number of beads.

To determine the torsion constant using a rotating magnetic field, the rotational movement of the beads has to be analyzed. The angular position of the bead in every captured frame can be determined by using a Matlab algorithm developed by [2], [8] and improved by Verhees [3]. The angular position of the bead is tracked as a function of time. The algorithm uses a computer-generated version of the first diffraction ring to determine the center of the bead. The diffraction ring is a bright concentric ring around the bead, as can be seen in Figure 4.5.

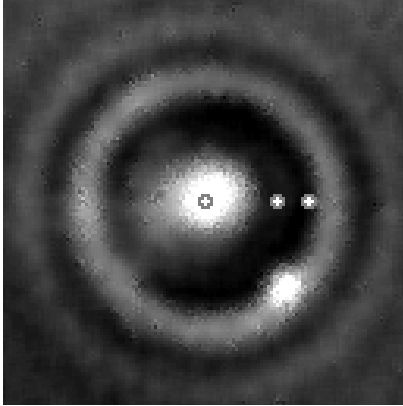


Figure 4. 5: Image of the bead captured with the microscope. The first and second diffraction rings are the concentric rings around the bead. The fluorescent label is also visible. The spot in the center represents the center of the bead. The two other spots are used to locate the fluorescent label and thereby track the bead rotation in every frame.

The inner and outer radius of the first diffraction ring are manually specified. The first image in frame sequence is used as a reference image. The cross-correlation for every other image with this reference image is calculated.

By using the time trace, the maximum angle over which the bound bead can rotate and the phase lag between the magnetic moment of the bead and the magnetic field can be determined. We considered an equilibrium angle situated exactly halfway between the maximum angle in clockwise rotation and the maximum angle in the anticlockwise rotation. The maximum angle is the largest angular deviation from the equilibrium. Figure 4.6 shows an example of the angular position of the beads a function of time obtained by using the Bead Rotationtracking Matlab script.

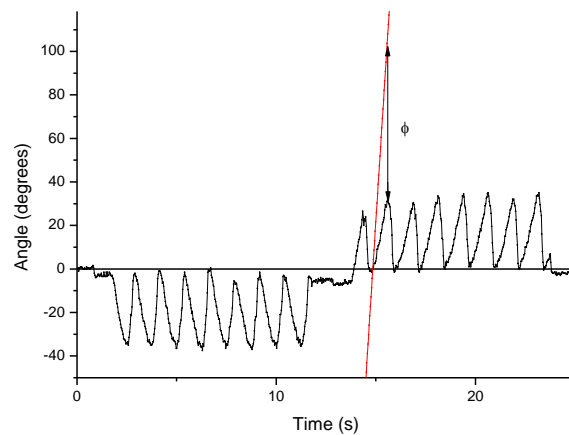


Figure 4. 6: Bead angular position as a function of time. The bead is bound via a G-IgG complex to a glass substrate in a 20 mT field rotating at 0.4 Hz. The red line represents the field in the anticlockwise direction. The field first rotates in the clockwise direction from 0 to 12 seconds, then after switching off the field the magnetic field in the anticlockwise direction is generated at second 14. The phase lag ϕ is the difference in angle between then magnetic field (red line) and the top of a oscillation.

5 Results and discussion

5.1 Dose response curve of Tn – anti-cTnI

The ultimate goal with the Tn – anti-TnI system is to perform torsional experiments to investigate structural properties of the complex. Only specific bonds of antibodies and troponin are useful for the rotation experiments and therefore a validation of the bead-based assay is required. To accomplish this a dose response curve is measured as described in the previous sections. The dose response curve of the sandwich assay for troponin is shown in Figure 5. 1.

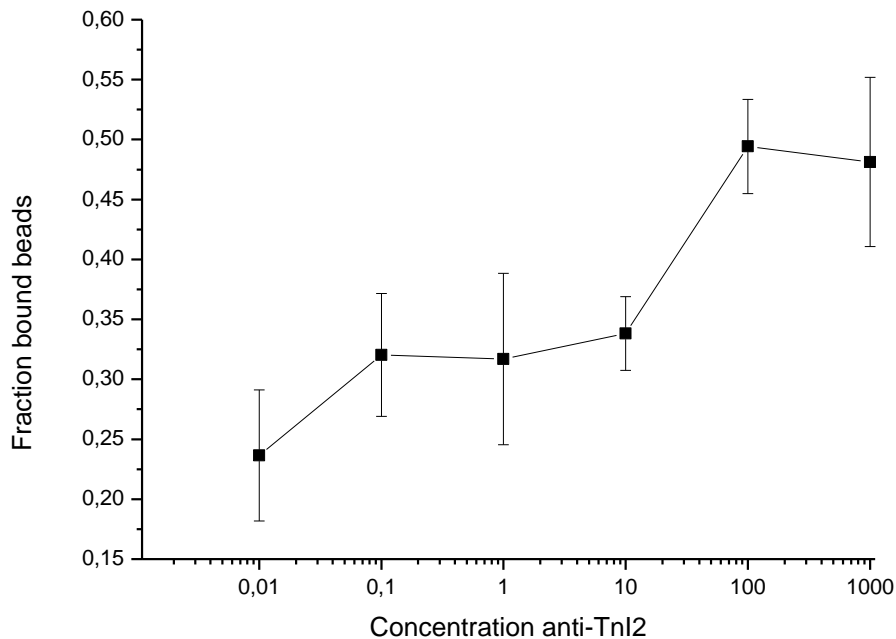


Figure 5. 1: Fraction of functionalized beads bound to the anti-TnI2 (HyTest 19C7) coated glass substrates as a function of the concentration of anti-TnI2.

From the graph of Figure 5. 1 it is concluded that the number of beads bound to a functionalized glass substrate increases with increasing concentration of anti-TnI2. This is expected because the functionalized substrate with low concentration of anti-TnI2 is not completely covered by the antibody molecules so that there are less places for troponin to bind specifically. At low concentration of anti-TnI2 no bonds should appear. The beads that do bind to the top substrate at very low concentration, for example 0.01 nM, can be bound via non-specific bonds. From the dose response curve above, there is a fraction of 0.23 bound beads at 0.01 nM. At high concentration of anti-TnI2 there is a higher coverage of the glass substrate so that the probability of the coated beads bind to the antibody is higher.

To minimize the bonds of the functionalized beads at low concentration of antibodies and to increase the fraction of bound beads at high concentration of the antibodies, polystyrene substrates are used instead of glass substrates. Figure 5. 2 gives the dose response curve of troponin system measured with functionalized polystyrene substrates.

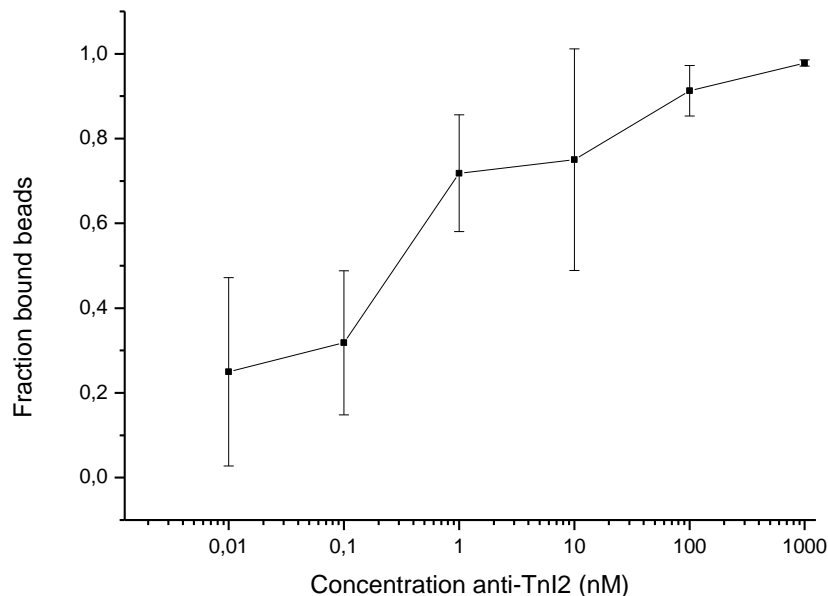


Figure 5. 2: Dose response curve of protein troponin obtained by using anti-TnI2 coated polystyrene substrates.

The fraction of bound beads goes up for increasing concentration of the anti-TnI2. In the case of the two highest anti-TnI2 concentrations almost all the functionalized beads bind to the coated substrate. This is expected because a higher anti-TnI2 concentration during the functionalization of the substrates could probably result in a higher coverage of the antibodies. Consequently there is a higher probability that the protein troponin on the M-270 beads binds to anti-TnI2 on the substrates.

At a concentration of 0.01 nM, 25% of beads bound to the surface. At this concentration we cannot determine whether the bonds formed are specific or non-specific because no control measurement – in which the substrates are not coated with the antibodies – were performed. Further validation and optimization of the assay is needed in order to use this system for torsion experiments.

5.2 Torsion constant of the protein G-IgG complex

The protein G-IgG complex is used for rotation experiments in this study. The experiments are performed to investigate the influence of surfactant on the torsion constant of the protein G-IgG complex. The torsion stiffness of the protein G-IgG complex is investigated in earlier studies ([1], [2] and [3]).

5.2.1 Determining the torsion constant of the G-IgG complex using rotational Brownian motion analysis

The torsion constant can be determined with a method which is based on the rotational Brownian motion analysis that is described in section 4.5. The rotational fluctuations of a bound bead in the absence of the magnetic field are shown in Figure 5.3.

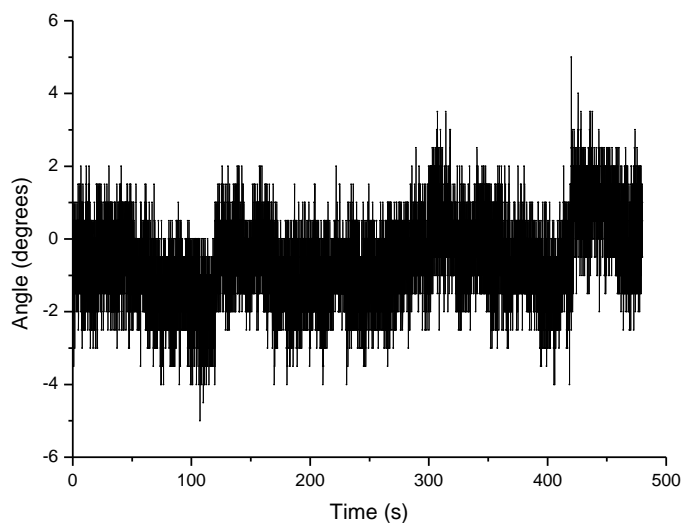


Figure 5. 3: Rotational fluctuations of a bound bead as a function of time.

The time trace of the rotational Brownian motion is used to determine the torsion constant. The angle as a function of time is translated into a histogram. The histogram is constructed with the Origin software package (OriginLab, Northampton, MA). The distribution function, equation (4.3) is used for the fitting process. The translated histogram from the time trace above can be seen in Figure 5. 4.

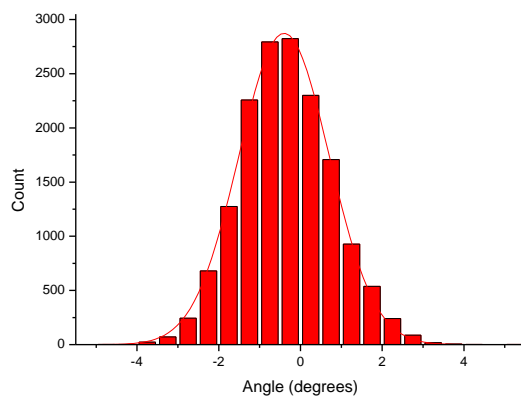


Figure 5. 4: The corresponding histogram of the angle of the time trace above. In order to determine the torsion constant, the histogram is fitted with eq (4.3)

From the fitting process, the torsion constant k of the protein complex is obtained. The rotational Brownian motion analysis is applied to a number of different beads to determine the torsion constant. In table 5.1 the torsion constants of different beads are shown.

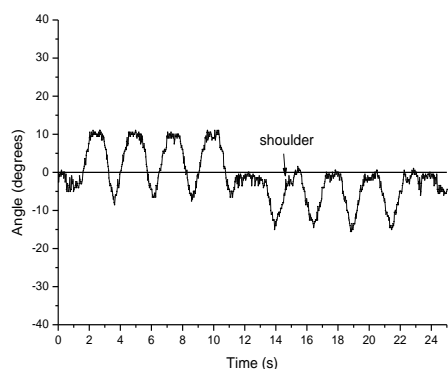
Table 5. 1: Measured torsion constants of different beads bound via the G-IgG complex. The torsion constant are determined with two methods described in section 4.5.

Bead	Torsion constant - Brownian motion ($\times 10^{-18} \text{ Nm} \cdot \text{ rad}^{-1}$)
1	12 ± 4.3
2	14 ± 3.3
3	11 ± 0.3
4	2.9 ± 0.6

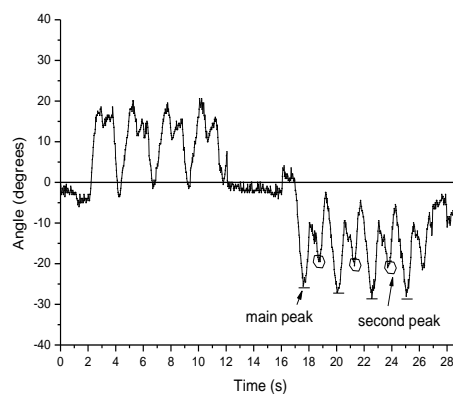
The torsion constants from the Brownian motion measurements have a variation, namely from $2.9 \text{ Nm} \cdot \text{ rad}^{-1}$ to $14 \text{ Nm} \cdot \text{ rad}^{-1}$. This variation is probably caused by the random orientation of the antibody on glass substrates. It cannot be excluded that the variation in torsion constant is caused by multiple bonds of the IgG molecules. The average torsion constants obtained from the Brownian measurements is $(10 \pm 2) \times 10^{-18} \text{ Nm} \cdot \text{ rad}^{-1}$. This value is almost twice the value that Verhees [3] found in his research, namely $(6 \pm 2) \times 10^{-18} \text{ Nm} \cdot \text{ rad}^{-1}$. But when errors are taken into account, the torsion constant obtained from the Brownian motion measurements can be comparable to the literature value. This indicates that the rotational Brownian motion analysis is a valid method for determining the torsion constant of a biological system.

5.2.2 Oscillating behavior and effect of magnetic field strength

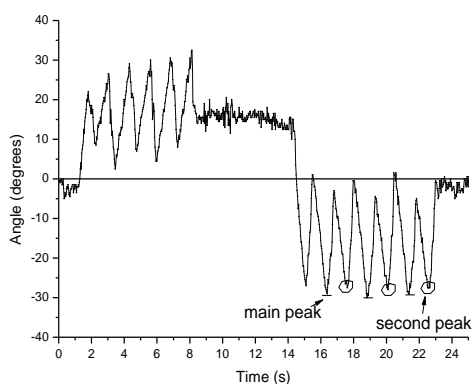
The rotation experiments are performed on glass substrates coated with 1 nM of IgG molecules. This is to decrease the probability of multiple bonds of the antibodies on the glass substrates. The frequency of the rotating magnetic field is kept constant at 0.4 Hz. The magnetic field strength is varied from 5 mT to 20 mT. The bead and sample preparation are described in sections 4.1 and 4.3. The angular deviation of one bound bead as a function of time is plotted for different field strengths in Figure 5.5



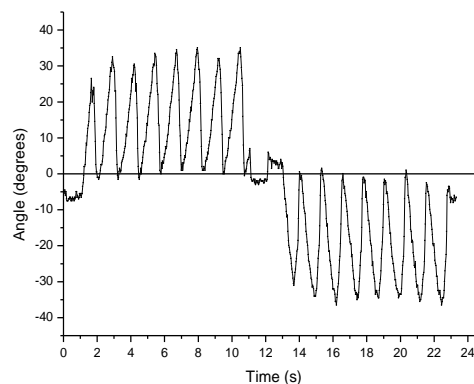
(a) 5 mT



(b) 10 mT



(c) 15 mT



(d) 20 mT

Figure 5. 5: The angular excursion of a bead bound via a protein G-IgG complex as a function of time. The measurement is repeated for four different rotating magnetic field strengths (a) 5 mT, (b) 10 mT, (c) 15 mT and (d) 20 mT. All the measurements are performed with clockwise and anti-clockwise rotation of the magnetic field. In (b) and (c), the short horizontal line on the top of the oscillation marks the main peaks while the secondary peaks are marked with circles.

The oscillation of the bound bead shows different behavior at different field strengths. To explain this, we consider that the bead has a distribution of magnetic grains with different sizes and orientation. At low field strength Figure 5.5a the rotation frequency of the bead is equal to the field frequency. According to our model this is the case when there is no remagnetization of the grains' moments since the external field is not large enough to exceed the coercive fields of the grains. Shoulders are visible in the measurement with an applied field of 5 mT. The shoulders appear due to the remagnetization of a small fraction of the grains' moments. The situation at 5 mT field is comparable to the described scenario 2 in section 2.4. When the first moment flipped, the phase lag between the effective magnetic moment and the field increases which can cause the next grain to flip sooner (note that this phase lag can be different from the phase lag between the magnetic moment and the field at maximum angle). Nevertheless this increased phase lag is not large enough such that more grains' moments can flip so that just a small fraction of the grains' magnetic moments are remagnetized. In Figure 5.5b when the field is increased to 10 mT the bead is still able to follow the field with the same frequency but shoulders are

more visible in the measurement. This indicates that the fraction of grains whose coercive field is exceeded increases. The flipping of a fraction of grains moments gives rise to the secondary oscillations. The secondary oscillations, resulted from the magnetization of the magnetic moment of grains, are denoted as secondary peaks.

In Figure 5.5c the secondary peaks are almost equal to the main peaks because the fraction of grains that remagnetized increases. This leads to larger oscillation amplitude of the secondary peaks. In Figure 5.5d it is observed that the bead frequency is 0.8 Hz which is twice the field frequency. This implies that the magnetic moment of the bead flips two times its orientations in one actual period of the field. Also worth noticed is that the secondary peaks cannot be distinguished from the main peaks anymore. The situation with 20 mT field is comparable to scenario 3 described in section 2.4. This means that the 20 mT magnetic field is high enough to exceed the coercive field of every grain in the distribution. In summary at the lowest field strength, the bead frequency is equal to the field frequency while at the highest field strength it is twice the field frequency. This implies that the coercive field of the magnetic moments is lower than 20 mT. At low field strength the bead has a difference in peaks, corresponding to the remagnetizing and non-remagnetizing fraction of the grains which originate from the differences in magnetic moments orientation of the grains coercivity. At high field strength, the difference is peaks is not observed anymore, which implies that all magnetic moments remagnetized.

For increasing field strengths, it is observed that the angular deviation from an equilibrium angle of the G-IgG system increases. This can be explained by using equation (4.1). With increasing magnetic field, the magnetic torque is increased as well. For increased magnetic torque, the equilibrium with the viscous and molecular spring torque is reached later, resulting a larger rotation angle. The effect of the field strength on the maximum rotation angle can be seen in Figure 5. 6.

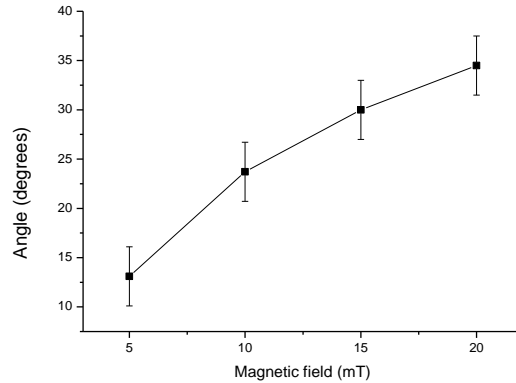


Figure 5. 6: The maximum rotation angle as a function of the applied magnetic field.

Further, the phase lag between magnetic torque and the magnetic field at the maximum angle is also studied. It is observed that the phase lag at maximum angle decreases for increasing field strength. This can be seen in Figure 5. 7.

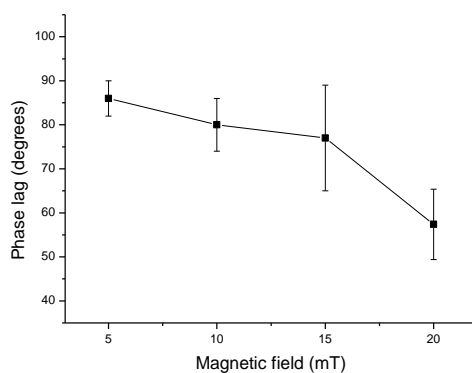


Figure 5. 7: Phase lag at maximum magnetic torque as a function of magnetic field strength.

As described in section 2.4, when a rotating magnetic field is applied, a few magnetic moments will flip. For increasing field, the remagnetization of these moments is reached sooner. When these moments remagnetize and cause a cascade effect, which is described in section 2.4, this might lead to a remagnetization of the effective magnetic moment and finally in backward rotation of the bead. When the remagnetization of the effective magnetic moment is reached sooner, the phase lag at maximum angle can be smaller than 90° .

5.2.3 The field dependence of the permanent magnetic moment and the angle dependence of the torsion constant

In this section the ratio between the torsion constant of the protein G-IgG complex and the permanent magnetic moment of the bead is determined by using a rotating magnetic field. For each measurement the phase lag is determined at the maximum angular deviation. By using equation (4.1) the ratios are calculated at different magnetic field strength.

The ratio between the torsion constant and the permanent magnetic moment as a function of the field strength is given in Figure 5. 9. The figure shows the graphs of three different beads.

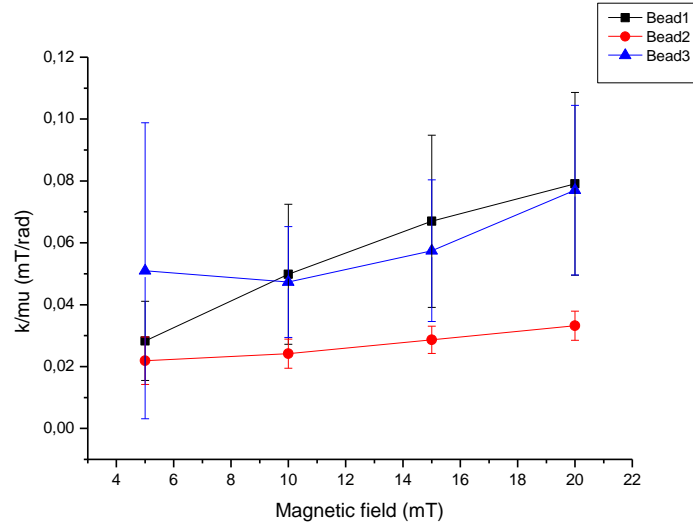


Figure 5. 8: The ratios between the torsion constant and the magnetic moment of three different beads as a function of the applied field. The lines are drawn to guide the eye.

The Figure 5. 8 above shows that the ratio between the torsion constant of the G-IgG complex and the permanent magnetic moment of the bead is not constant for increasing magnetic field strength. The ratio is increased for increasing field strength. This can be caused by two reasons: either the torsion constant or the magnetic moment of the bead are not constant .

In the first case, a fixed torsion constant is assumed. The magnetic moment of the bead can be determined by using equation (4.1) and the torsion constant obtained from the Brownian motion measurements described in section 5.2.1. The magnetic moments of three different beads as a function of the applied field are show in Figure 5. 9.

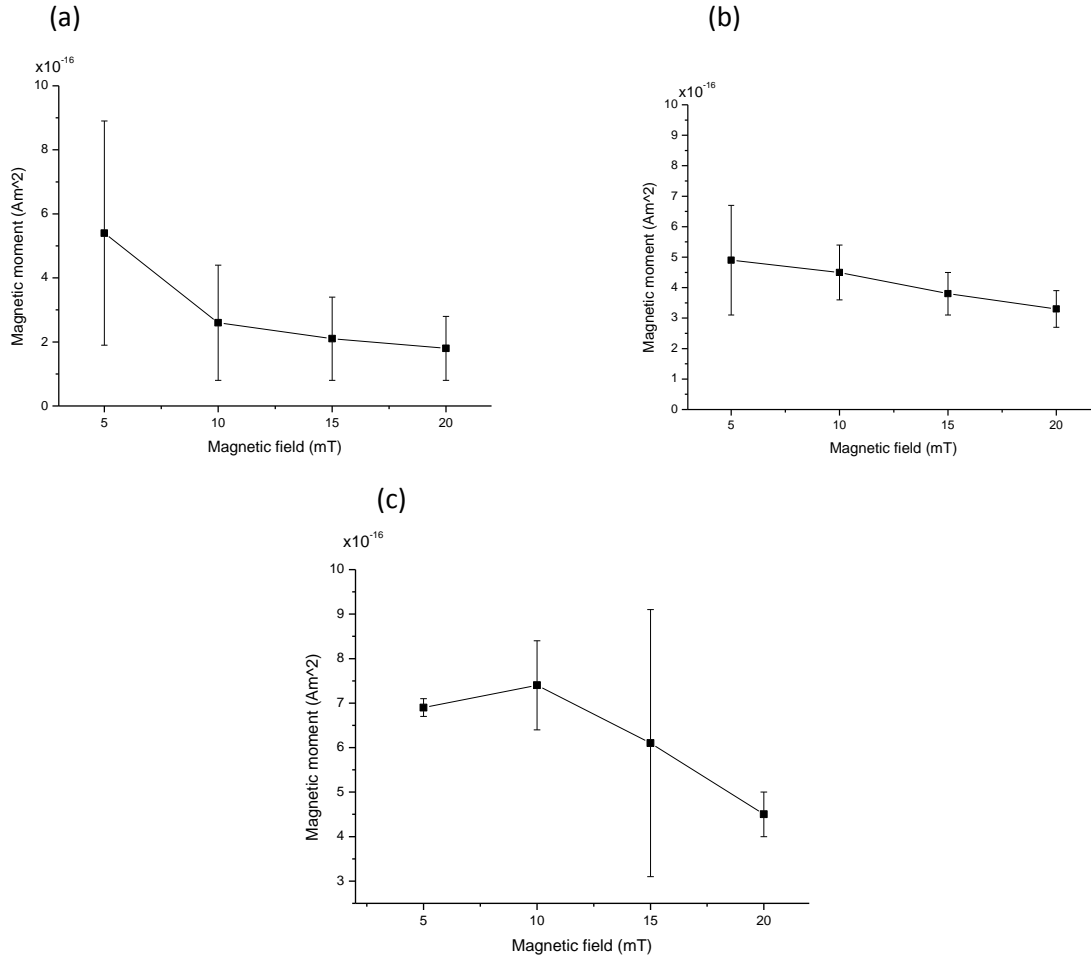


Figure 5. 9: The permanent magnetic moment of three different beads as a function of the magnetic field strength. The torsion constants are obtained from the rotational Brownian motion analysis. In (a) the torsion constant is fixed at $k= (14 \pm 3.3) \times 10^{-18} \text{ Nmrad}^{-1}$, in (b) $k= (11 \pm 0.3) \times 10^{-18} \text{ Nmrad}^{-1}$ and in (c) $k= (35 \pm 28) \times 10^{-18} \text{ Nmrad}^{-1}$. The lines are draw to guide the eye.

When considering the three beads in Figure 5. 9 a general trend can be seen. The magnetic moment is reduced for increasing field. The obtained magnetic moments are measured where the flipping of the grains is present. During the measurement the phase lag at maximum angle between the effective magnetic moment and the field is not fixed due to the cascade effect described in section 2.4. Figure 5. 7 shows that the phase lag decreases for increasing field, which can explain the decreasing of magnetic moment when a fixed torsion constant is considered. A decreasing of magnetic moment results in a increasing of the ratio between the torsion constant and the magnetic moment.

In the second case, a constant magnetic moment is assumed. The torsion constant is calculate with equation (4.1). The torsion constant of three different beads as a function of the maximum angle is shown in Figure 5. 10.

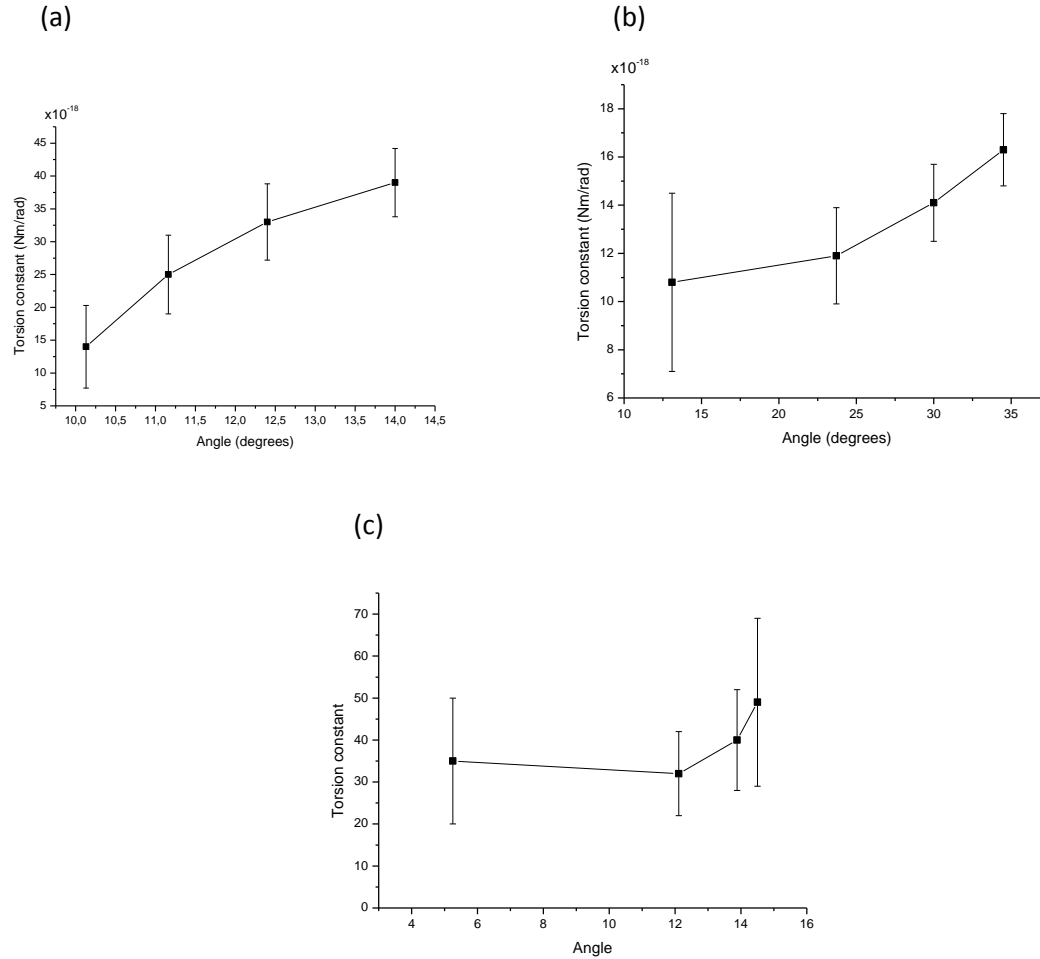


Figure 5. 10: The torsion constant of three different beads as a function of the maximum angle. The torsion constant is calculated with equation (4.1). The magnetic moment in (a) is $\mu = (5 \pm 3.1) \times 10^{-16} \text{Am}^2$, (b) $\mu = (4.9 \pm 1.9) \times 10^{-16} \text{Am}^2$ and (c) $(6.9 \pm 0.2) \times 10^{-16} \text{Am}^2$.

From the graphs above, a trend can be seen. The torsion constant increases for increasing angle. With the method using a rotating magnetic field, we found that the torsion constant of the protein G-IgG complex depends on the rotation angle. Compare to the average torsion constant obtained from the rotational Brownian motion analysis, which is $(10 \pm 2) \times 10^{-18} \text{Nm} \cdot \text{rad}^{-1}$, the values at 5 mT field from (a) and (b) have overlapping within the error margin.

The two cases described above are cases in which one of the parameter is considered to be constant. It cannot be excluded that both the magnetic moment and the torsion constant are dependent on the field strength. Further investigations will be needed to gain more knowledge about the magnetic moment of the bead and the torsion constant.

5.2.4 Influence of surfactant on the torsion constant of the protein G-IgG complex

To study the influence of surfactant on mechanical properties of biological system, the torsion constant of protein G-IgG complex is determined first without surfactant added in the PBS solution, then with surfactant in the solution. Sodium dodecyl sulfate (SDS) different concentrations respect the CMC,

namely 0.1xCMC and 1xCMC, are used in the experiments. Determining of torsion constant is based on the methods with rotating magnetic field and rotational Brownian motion analysis.

Figure 5. 11 shows the angular deviation in the presence of a as a function of time of one bead for measurement with and without surfactant SDS with 1xCMC.

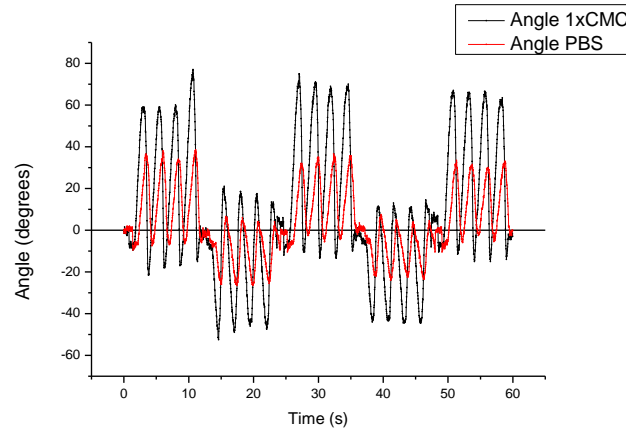


Figure 5. 11: The angular position of a bound bead measured in PBS (red) and in PBS with SDS with 1xCMC (black). The measurement is performed with a magnetic field strength of 5 mT.

From Figure 5. 11, it is observed that after adding surfactant the angular deviation increases. The increasing in maximum angle is found to be dependent on the concentration of SDS. The fraction $\frac{\theta_{SDS} - \theta_{PBS}}{\theta_{PBS}}$ quantifies the relative change in flexibility for a single bead. This fraction has an average of 0.25 for solutions of 0.1xCMC and 0.7 for solutions with 1xCMC. This results reveals that the protein flexibility increases with the concentration of surfactant.

The torsion constants are measured and presented in Table 5. 2.

Table 5. 2: Overview of torsion constants ($\times 10^{-18} \text{ Nm} \cdot \text{rad}^{-1}$) measured with rotating magnetic field and Brownian motion (for bead4 and bead5). For the same bead, experiments are performed in PBS solution with and without surfactant.

Bead1-PBS	3.9 ± 1.5
Bead1-SDS 0.1xCMC	2.3 ± 1.1
Bead2-PBS	1.5 ± 0.4
Bead2-SDS 0.1xCMC	1.4 ± 0.4
Bead3-PBS	1.8 ± 0.4
Bead3-SDS 0.1xCMC	1.4 ± 0.3
Bead4-PBS	4.3 ± 0.6
Bead4-SDS 1xCMC	3.1 ± 0.5
Bead4-SDS 1xCMC Brownian motion	3.1 ± 0.3
Bead5-PBS	11 ± 4.6
Bead5-SDS 1xCMC	7 ± 1.5
Bead5-SDS 1xCMC Brownian motion	8.7 ± 0.1

From the results of the performed experiment, it is concluded that surfactant decreases the torsion constant of the protein G-IgG complex. The biological system becomes less rigid under influence of surfactant. For bead4 and bead5 in solution with SDS with 1xCMC their torsion constants are also

determined with the rotational Brownian motion as can be seen in Table 5. 2. The torsion constants measured with the Brownian motion are in agreement with the ones obtained from measurements with magnetic field.

6 Conclusions and outlook

In this research the Troponin – Anti-troponin complex in particle-based immunoassay is investigated for posterior use in torsion experiments. The cardiac troponin ICT complex is sandwiched between anti-troponin I1 and a substrate coated with anti-troponin I2. The dose response curve of the complex is measured. From the dose response curve, a fraction of 0.25 of bonds at low concentration (0.01 nM) of antibodies is observed. We cannot be sure if these bonds are specific or non-specific. Therefore, the Troponin – Anti-troponin complex was not used for the rotational experiments. To minimize the fraction of bonds at low concentration of antibodies, experiments can be performed using another blocking agents, e.g. casein or PEG polymers.

The protein G-IgG complex is used for the torsion experiments. The torsion constant of the G-IgG complex is determined with a method which is based on the angular Brownian motion analysis. For different beads, the value of the torsions constant varies from $2.9 \text{ Nm} \cdot \text{rad}^{-1}$ to $14 \text{ Nm} \cdot \text{rad}^{-1}$. This variation can be caused mainly by: differences in orientation of the bonds between the substrate and the bead and multiple formation of bonds. The average torsion constant found with this method is $(10 \pm 2) \text{ Nm} \cdot \text{rad}^{-1}$. This average torsion constant is comparable to the literature value which is $(6 \pm 2) \times 10^{-18} \text{ Nm} \cdot \text{rad}^{-1}$. The determination of the torsion constant with the rotational Brownian motion analysis can be improved if we can control the orientation of the antibodies on the substrate and reduce multiple bonds of antibodies.

The twisting behavior of the protein G-IgG complex is studied by applying a rotating magnetic field with different field strengths ranging from 5 to 20 mT. In general at low magnetic field strength the bead frequency is equal to the field frequency. At intermediate field the oscillation started to show shoulders. At high field strength a twofold bead frequency appeared with respect to the field frequency. To explain these behaviors a distribution of magnetic grains with different size and orientation is considered. These results can give additional insight in the structural properties of the magnetic beads.

The bead angle increased with increasing magnetic field strength due to increasing magnetic torque. For a larger torque the equilibrium between the viscous and molecular spring torque is reached later in the rotation cycle which causes a larger rotation angle.

The ratio between the torsion constant and the magnetic moment of the bead is not constant for different field strengths. It is observed that the ratio increased for increasing field strength. We did not find an explanation for this effect. A satisfactory explanation is yet to be found. Still we have considered two cases where the torsion constant is kept constant in the first case and in the second case, the magnetic moment is fixed. In the first case, the magnetic moment is calculated when flipping of the grains is present. Due to the flipping, the phase lag between the magnetic moment and the field is not fixed which can cause the magnetic moment to change as a function of the field strength. In the second case, the torsion constant is determined by using the maximum angle of the bead. This angle is dependent on the magnetic field strength which causes the field dependence of the torsion constant.

At last, the conformational changes of the protein G-IgG complex upon exposure to surfactant is also studied. It is observed that after adding SDS in the solution, the bead angle increased. Also the torsion constant of the complex decreased after adding SDS in the solution. It is concluded that surfactant decreases the rigidity of the G-IgG system. One possible explanation for this is that surfactant changes the structure of the protein complex but more data is needed in order to confirm this statement.

7 References

- [1] J.M. van Noorloos. Measuring the torsion stiffness of the protein G-IgG complex. Master thesis applied physics, Eindhoven University of Technology, 2009.
- [2] A. van Reenen. Twisting protein by magnetic particle actuation. Master thesis, Eindhoven University of Technology, 2010.
- [3] L.J.P. Verhees. A magnetic particle based study of twisting the protein G-IgG complex. Master thesis, Eindhoven University of Technology, 2013.
- [4] X.J.A. Janssen, A.J.Schellekens, K.Van Ommering, L.J.Van Ijzendoorn, and M.W.J.Prins. Controlled torque on superparamagnetic beads for functional biosensors. *Biosens. Bioelectron.*, 24(7):1937-1941, 2009.
- [5] J.P. Davis, S.B.Tikunova. Ca^{2+} exchange with troponin C and cardiac muscle dynamics. *Cardiovascular Research*, 77: 619-626, 2008.
- [6] A. E. Sauer-Eriksson, G. J. Kleytwegt, M. Uhlén, T. A. Jones. Crystal structure of the C2 fragment of streptococcal protein G in complex with the Fc domain of human IgG. *Structure* 3: 265-278, 1995.
- [7] M. Zantema. Juggling with beads: Software for controlled rotation of beads. Bachelor thesis, Eindhoven University of Technology.
- [8] B. de Clerq. Probing biological bonds by means of rotation of superparamagnetic beads. Master's thesis, Eindhoven University of Technology, 2008.

8 Appendix

A1. Bead coating with anti-troponin

Materials:

Buffers:

- PBS buffer 0.01 M (1 tablet per 200 ml demi water)
- Coupling buffer: MES buffer 100mM, pH 5
- Activation buffer: 3 mg EDC, 3 mg NHS in 50 µl MES buffer 25mM, pH 5
- Wash buffer: PBS pH 7.4 containing 0.5% BSA and 0.01% Tween-20
- Storage buffer: PBS pH 7.4 containing 0.5% BSA and 0.01% Tween-20
- Assay buffer: PBS pH 7.4 containing 1% BSA and 0.02% Tween-20
- Ethanolamine: 50mM, prepared in PBS, pH 8

Particles:

- Dynabeads M-270 Carboxylic Acid (stock = 2E9 beads/ml)

Proteins:

- 0.1 µM anti-TnI (HyTest 560, 4.6 mg/ml), diluted in 100mM MES, pH 5
- 10 nM Tn-IC protein complex (HyTest 8IC63), diluted in assay buffer, pH 7.4 150 mM

Miscellaneous:

- Low Bind Eppendorf tubes
- (On the day of measurements) Ice to store the Troponin protein complex

Methods:

1. After gently shaking the bottle containing the beads (shake to get a homogenous suspension), pipette out 2 µl beads. Add 198 µl demi and mix well.
2. Pipet the supernatant into an Eppendorf tube. Dispose it in the toxic waste.
3. Wash the beads 5 times in 200 µl MES buffer, 25mM, pH 5. Vortex in between the washes to resuspend the pellet.
4. Remove the supernatant again and resuspend the beads in 40 µl activation buffer. Let the EDC and NHS incubate at room temperature for 45 minutes while vortexing the Eppendorf at 1400 RPM.
5. Remove supernatant and add 30 µl 10 nM anti-TnC. Incubate at 4° for 2 hours by vortexing at 1400 RPM. Take care that the solution stays at the bottom of the tube.
6. Remove supernatant and immediately add 100 µl cold ethanolamine. Vortex for 30 minutes at 1400 RPM.
7. Wash 4 times with 200 µl wash buffer. Vortex well between each wash.
8. The beads can now be stored at 4 degrees in 200 µl storage buffer.
9. Add 10 µl 1 nM Tn-IC protein complex (diluted with assay buffer, pH 7.4) to 40 µl functionalized beads.
10. Centrifuge for 2 minutes at 14300 RPM and vortex 3 minutes at 1400 RPM. Repeat this 1 more time.

11. Magnetically wash 2 times with assay buffer to remove the excess of unbound Tn-IC protein complex.
12. Check whether (large) clusters are present in the bead solution. Apply sonication if necessary.

A2. Samples preparation for troponin experiments

Materials:

Buffers:

- PBS buffer 0.01 M (1 tablet per 200 ml demi water)
- Block buffer: 100 mM PBS with 10% BSA
- Antibody buffer: anti-cTnI (HyTest 19C7), diluted in 100mM MES, pH 5

Miscellaneous:

- Glass coverslips (for example 18x18 mm) and spacers

Methods:

1. Wash the glass coverslips (for example by sonication in an acetone solution for 5 minutes, followed by sonication in an isopropanol solution for 5 minutes). Dry by using a vacuum desiccator for 5 minutes.
2. Prepare an open fluid cell consisting of a glass cover slip and a spacer attached to it.
3. Incubate 100 μ l anti-cTnI buffer on each substrate for 45 minutes.
4. Remove the remaining droplet using a pipette and wash by pipetting in and out PBS buffer for 2 times.
5. Incubate 100 μ l block buffer on each substrate for 1 hour.
6. Wash the fluid cells by moving the sample back and forth in a beaker filled with PBS using tweezers for about 30 seconds. The normal on the plane of the substrate should be directed horizontally.
7. Dry the remaining fluid outside the imaging spacer with a tissue. Don't touch the area inside the imaging spacer.

Just before measuring the samples:

1. Pipette 8.5 μ l of the bead suspension (coated with anti-TnC and Tn-IC) on a new washed glass cover slip. Subsequently turn it upside down and place it on the cover slip with the imaging spacer so that the beads sediment to the antibody coated surface.
2. Let the coated beads incubate on the antibody coated substrate for 3 minutes. Then turn the sample upside down (so that the functionalized substrate with the bound beads is located on top) and let the unbound beads sediment (by gravity) for another 3 minutes. Now the unbound beads will be separated from the bound beads.

A3. Bead coating with protein G

Materials:

Buffers:

- PBS buffer 0.01 M (1 tablet per 200 ml demi water)
- Coupling buffer: MES buffer 100mM, pH 5
- Activation buffer: 3 mg EDC, 3 mg NHS in 50 µl MES buffer 25mM, pH 5
- Wash buffer: PBS pH 7.4 containing 0.5% BSA and 0.01% Tween-20
- Storage buffer: PBS pH 7.4 containing 0.5% BSA and 0.01% Tween-20
- Assay buffer: PBS pH 7.4 containing 1% BSA and 0.02% Tween-20
- Ethanolamine: 50mM, prepared in PBS, pH 8
- Dynabeads M-270 Carboxylic Acid (stock = 2E9 beads/ml)
- 0.14 µM recombinant protein G diluted in PBS buffer 100 mM
- 0.03 µM streptavidin diluted in PBS buffer 100 mM
- Low Bind Eppendorf tubes

Methods:

1. After gently shaking the bottle containing the beads (shake to get a homogenous suspension), pipette out 2 µl beads. Add 198 µl demi and mix well.
2. Centrifuge the beads. Pipette the supernatant (manufacturer's buffer containing sodium azide) into an Eppendorf tube. Dispose it in the toxic waste.
3. Wash the beads 5 times in 200 µl 100 mM PBS buffer. Vortex in between the washes to resuspend the pellet.
4. Remove the supernatant again and resuspend the beads in 40 µl activation buffer. Let the EDC and NHS incubate at room temperature for 45 minutes while vortexing the Eppendorf at 1400 RPM.
5. Remove supernatant and add 100µl 0.14 µM recombinant protein G followed by 100 µl 0.03 µM streptavidin. Incubate at 4° for 2 hours by vortexing at 1400 RPM. Take care that the solution stays at the bottom of the tube.
6. After incubation, centrifuge the beads and pipette out the biomolecule solution.
7. Immediately add 400 µl 50 mM cold ethanolamine. Vortex for 1 hour at 1400 RPM.
8. Wash 4 times with 200 µl wash buffer. Vortex well between each wash.
9. Resuspend the beads in 200 µl storage buffer. Observe the beads under the microscope. If no aggregation is seen the beads can be stored at 4°.

A4 Fluorescent labeling of streptavidin coated beads

Materials:

- Dynabeads M-270 Carboxylic Acid coated with streptavidin and protein G according to the protocol in A3.
- FluorSpheres biontin-labelled microspheres yellow-green fluorescent, Molecular Probes.
- Assay buffer: 1 ml 100 mM PBS, 1% BSA, 0.02% Tween-20

Method

1. Prepare a 100 times dilution of the fluorescent beads by using 198 μl demi water to 2 μl stock fluorescent bead solution. Use a Low Bind Eppendorf tube.
2. Optionally remove the bead clusters by applying a short 0.2s sonic pulse
3. Replace the storage buffer in the bead solution by demi water.
4. Add 7 μl fluorescent bead solution to 56 μl of the streptavidin coated M-270 bead suspension. Mix well by vortexing.
5. Centrifuge the beads for 5 minutes at 13400 rpm.
6. Resuspend the beads by vortexing for 10 minutes.

A5 Sample preparation with IgG coated surface

Material:

- Glass cover slips and fluid cell
- Synthetic grease
- Dynabeads M-270 Carboxylic Acid coated with streptavidin and protein G according to the protocol in A3.
- FluorSpheres biontin-labelled microspheres yellow-green fluorescent, Molecular Probes.
- Assay buffer: PBS pH 7.4 containing 1% BSA and 0.02% Tween-20.
- Block buffer: 100 mM PBS with 10% BSA.
- IgG buffer: 100 μl 1 nM IgG in 100 mM PBS.

Method

1. Wash the glass cover slips with acetone and isopropanol and dry by using a vacuum desiccators.
2. Incubate 100 μl IgG buffer on each substrate for 45 minutes.
3. Remove the remaining droplet by using a pipette and wash by pipetting in and out PBS buffer for 2 times.
4. Incubate 100 μl block buffer on each substrate for 1 hour.
5. Wash the fluid cell by moving the sample up and down with tweezers in a beaker filled with PBS for 30s. The normal on the plane of the substrate should be directed horizontally.
6. Just before use, label 56 μl of the prepared bead suspension with fluorescent labels according to protocol A4.
7. Pipette 45 μl of the bead suspension on the glass substrate coated with IgG.
8. Put the sample on the magnetic quadrupole and immediately switch a static incubation field of 2 mT. Let the beads incubate for 10 minutes.
9. Glue a new washed glass substrate on the back of the fluid holder.
10. After incubation, turn the substrate with bead suspension upside down and put it on top of the open fluid cell. Unbound beads will now sediment due to gravity. The protein G-IgG bound beads can be visualized by focusing the microscope on the plane of the IgG functionalized surface.

